

# Collisional deexcitation of the excited rare gas atoms in resonant states: The Watanabe–Katsuura theory revisited

Hironobu Fukuzawa, Makoto Murata, Naoharu Kiyoto, Tomonori Mukai, Yuji Fukuchi,  
and Deba Bahadur Khadka

*Department of Chemistry, Tokyo Institute of Technology, Meguro-ku, Tokyo 152-8551, Japan*

Masatoshi Ukai

*Department of Applied Physics, Tokyo University of Agriculture and Technology, Koganei-shi,  
Tokyo 184-8588, Japan*

Takeshi Odagiri, Kosei Kameta, Noriyuki Kouchi,<sup>a)</sup> and Yoshihiko Hatano<sup>b)</sup>

*Department of Chemistry, Tokyo Institute of Technology, Meguro-ku, Tokyo 152-8551, Japan*

(Received 2 July 2002; accepted 7 October 2002)

The cross sections for the collisional deexcitation of neon atoms in the lowest excited  $^1P_1$  state by Ar, Kr, Xe,  $N_2$ ,  $O_2$ , CO, NO, and  $CH_4$ , and in the lowest excited  $^3P_1$  state by  $O_2$  and  $CH_4$  have been measured at a mean collisional energy corresponding to room temperature. Data are also included for collisions of argon atoms in the lowest excited  $^1P_1$  and  $^3P_1$  states by  $C_2H_4$ , *cyclo*- $C_3H_6$ , and  $C_3H_8$ , and collisions of krypton atoms in the lowest excited  $^1P_1$  and  $^3P_1$  states by  $C_2H_4$  and *cyclo*- $C_3H_6$ . The measured cross sections, together with those obtained in our previous studies, are compared with the cross sections calculated using the Watanabe–Katsuura theory. An extension of the Watanabe–Katsuura theory to the deexcitation of excited rare gas atoms in collisions with molecular quenchers, not atoms, is examined. © 2003 American Institute of Physics. [DOI: 10.1063/1.1524626]

## I. INTRODUCTION

Collisional deexcitation of excited rare gas atoms by atoms and molecules is of great importance in both fundamental and applied sciences. It is well known that the Watanabe–Katsuura theory (WK theory)<sup>1</sup> is a simple and useful means to calculate the cross sections for Penning ionization in collisions between excited rare gas atoms in resonant states and atoms, which plays an important role in the deexcitation processes.<sup>2–4</sup> The advantage of the WK theory is that we need only two quantities to calculate the cross sections, i.e., the oscillator strength of the transition in the rare gas atom and the corresponding photoionization cross section of the atom used as a quencher, as shown in Eqs. (6)–(8). It should be noted that in the case of molecular quenchers non-ionization processes, such as dissociative excitation transfer, may play a role in deexcitation in addition to Penning ionization.<sup>5,6</sup> Thus it seems pertinent to apply the WK theory to collisional deexcitation by a molecule with the use of a photoabsorption cross section instead of a photoionization cross section (see also Ref. 7). This extension of the WK theory, however, has not been previously discussed in detail from either an experimental or theoretical point of view to the best of our knowledge.

In the present study, we have measured the cross sections for collisional deexcitation of excited rare gas atoms in resonant states by a wide range of atoms and molecules, for

which the photoionization quantum yields<sup>6</sup> at the energies characteristic of the excited rare gas atomic levels vary over a wide range, i.e., from zero to unity, in order to examine the extension of the WK theory in terms of experiments. The deexcitation cross sections measured in the present experiments, together with those determined for other collision systems in our previous experiments, are compared with two WK cross sections, i.e., one calculated using the photoionization cross section and the other the photoabsorption cross section, the former corresponding to the original WK theory, the latter to the extended one proposed here.

## II. EXPERIMENT

The experiments were carried out using the pulse radiolysis method incorporating time-resolved optical absorption spectroscopy.<sup>2,3</sup> In this work we have measured the cross sections for deexcitation of:

- the lowest excited  $Ne(^1P_1)$  atom by collisions with Ar, Kr, Xe,  $N_2$ ,  $O_2$ , CO, NO, and  $CH_4$ ;
- the lowest excited  $Ne(^3P_1)$  atom by  $O_2$  and  $CH_4$ ;
- the lowest excited  $Ar(^1P_1, ^3P_1)$  atoms by  $C_2H_4$ , *cyclo*- $C_3H_6$ , and  $C_3H_8$ ;
- the lowest excited  $Kr(^1P_1, ^3P_1)$  atoms by  $C_2H_4$  and *cyclo*- $C_3H_6$

at room temperature. In these collision systems, except for  $Kr(^3P_1)$ – $C_2H_4$  and *cyclo*- $C_3H_6$ , the excitation energies of the excited rare gas atoms exceed the first adiabatic ionization potentials of the quencher atoms and molecules,<sup>8,9</sup> and hence Penning ionization can energetically occur. After irra-

<sup>a)</sup>Author to whom correspondence should be addressed. Fax: +81-3-5734-2655. Electronic mail: nkouchi@chem.titech.ac.jp

<sup>b)</sup>Present address: Department of Molecular and Material Sciences, Kyusyu University, Kasuga-shi, Fukuoka 816-8580, Japan.

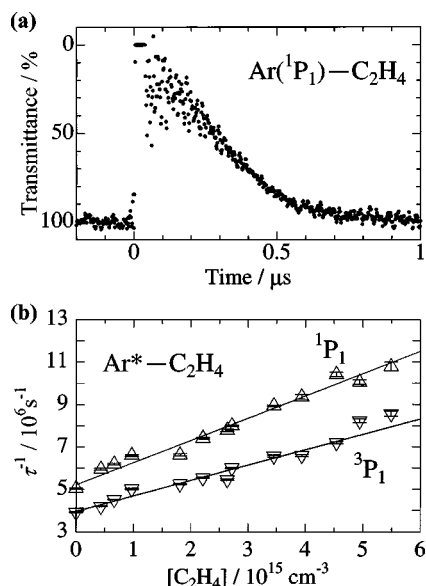


FIG. 1. (a) An example of the time-resolved transmittance. The absorption is due to the transition of  $\text{Ar}(4s^1P_1 \rightarrow 4p^1S_0)$  (750.3 nm) at room temperature in a mixture of Ar at 80 Torr,  $\text{C}_2\text{H}_4$  at 0.083 Torr, and  $\text{SF}_6$  at 0.20 Torr. (b) An example of the plots of  $\tau^{-1}$  vs  $[\text{M}]$  at room temperature, where  $\tau^{-1}$  is the decay rate of the lowest excited  $\text{Ar}(^1P_1, ^3P_1)$  atoms and the quencher M is  $\text{C}_2\text{H}_4$ . See Eq. (4). A mixture of Ar at 80 Torr,  $\text{C}_2\text{H}_4$  at 0–0.17 Torr and  $\text{SF}_6$  at 0.20 Torr.

diation by an intense nanosecond electron beam pulse onto a mixture of a rare gas with a trace amount of  $\text{SF}_6$  and a quencher, M, in a gas cell, time-resolved optical absorption associated with the excited Ne, Ar, or Kr atoms mentioned above was measured. The relevant transitions are listed below as well as their wavelengths:  $\text{Ne}(3s^1P_1 \rightarrow 3p^1S_0)$  (585.25 nm),  $\text{Ne}(3s^3P_1 \rightarrow 3p^3P_0)$  (607.43 nm),  $\text{Ar}(4s^1P_1 \rightarrow 4p^1S_0)$  (750.3 nm),  $\text{Ar}(4s^3P_1 \rightarrow 4p^3P_2)$  (738.3 nm),  $\text{Kr}(5s^1P_1 \rightarrow 5p^1S_0)$  (768.5 nm) and  $\text{Kr}(5s^3P_1 \rightarrow 5p^3S_0)$  (758.7 nm). The time-resolved absorption signal was converted to the density of the excited rare gas atoms as a function of time by using the absorption law mentioned elsewhere.<sup>2,3</sup> The time resolution of the whole system was approximately a few ns, which was estimated from the rising part of the observed signals. A trace amount of  $\text{SF}_6$  was added to remove thermal electrons produced in the irradiated sample gases, since they cause the collisional mixing among the atomic levels in the multiplet terms of interest and the emission of the fluorescences with the transitions from higher excited states to the lowest excited states of rare gas atoms following the recombination of the atomic ions with the thermal electrons.<sup>2,3,10,15,18</sup> An example of the time-resolved absorption signal is seen in Fig. 1(a).

The sample gases used are commercially available (special grade or research grade from Takachiho Co., Ltd.), and the *cyclo*- $\text{C}_3\text{H}_6$  gas had the lowest purity of 99.5 % among them. The gas mixtures consist of rare gases at tens to hundreds of Torr,  $\text{SF}_6$  at 0.1–0.2 Torr, and the quencher gas at 0 to  $\sim 0.5$  Torr.

### III. RESULTS AND DISCUSSION

In the present experiment, the following reactions dominate the deexcitation of the excited rare gas atoms,  $\text{Rg}^*$



where  $\tau_0$  is the effective lifetime of  $\text{Rg}^*$  in pure Rg, and  $k_{\text{SF}_6}$  and  $k_{\text{M}}$  are the rate constants for deexcitation of  $\text{Rg}^*$  by  $\text{SF}_6$  and M, respectively. Thus the density of the excited rare gas atoms as a function of time shows the first-order decay, and its decay rate,  $\tau^{-1}$ , is given by

$$\tau^{-1} = \tau_0^{-1} + k_{\text{SF}_6}[\text{SF}_6] + k_{\text{M}}[\text{M}], \quad (4)$$

where  $[\text{SF}_6]$  and  $[\text{M}]$  are the number densities of  $\text{SF}_6$  and M, respectively. The value of  $k_{\text{M}}$  is given by the slope of the straight line in the plot of  $\tau^{-1}$  vs  $[\text{M}]$  at a constant  $[\text{SF}_6]$  and constant pressure of rare gas. An example of such plots is seen in Fig. 1(b). A value of  $k_{\text{M}}$  is then converted to a value of velocity averaged cross section for the deexcitation of  $\text{Rg}^*$  by M,  $\sigma_{\text{M}}$ , at a mean collisional energy,  $E = (\frac{3}{2})k_{\text{B}}T$ , as

$$\sigma_{\text{M}} = k_{\text{M}}(\pi\mu/8k_{\text{B}}T)^{1/2}, \quad (5)$$

where  $k_{\text{B}}$ ,  $\mu$ , and  $T$  are the Boltzmann constant, the reduced mass of  $\text{Rg}-\text{M}$ , and the absolute temperature of the sample gas mixture, respectively. Note that in the present experiment target gases are at room temperature.

The cross sections obtained in the present measurement are listed in Table I together with the previous results<sup>10–13</sup> if available. The present and previous results are in agreement with each other.

As mentioned before, Watanabe and Katsuura<sup>1</sup> proposed a theoretical formula for the cross section for Penning ionization,  $A^* + B \rightarrow A + B^+ + e^-$ , due to a long-range dipole–dipole interaction. The theoretical cross section,  $\sigma_{\text{WK}}$ , is given by

$$\sigma_{\text{WK}} = 13.88 \left( \frac{M_A^2 \frac{dM_B^2}{dE}}{v} \right)^{2/5} \text{ (in a.u.)}, \quad (6)$$

where  $M_A^2$  and  $dM_B^2/dE$  are the transition dipole matrix elements squared for  $A \rightarrow A^*$  and  $B \rightarrow B^+ + e^-$  at the excitation energy of  $A^*$ , respectively,  $v$  the relative velocity between  $A^*$  and  $B$ , and a.u. stands for the atomic units.  $M_A^2$  and  $dM_B^2/dE$  are related to the oscillator strength and photoionization cross section by

$$M_A^2 \text{ (in a.u.)} = \frac{R}{E^*} f_A \quad (7)$$

and

$$\frac{dM_B^2}{dE} \text{ (in a.u.)} = \frac{2R/E^*}{4\pi^2\alpha a_0^2} \sigma_i, \quad (8)$$

where  $R$ ,  $\alpha$ ,  $a_0$ ,  $E^*$ ,  $f_A$ , and  $\sigma_i$  are the Rydberg energy, the fine structure constant, the Bohr radius, the excitation energy

TABLE I. Cross sections for deexcitation of the lowest excited  $\text{Ne}(^1P_1, ^3P_1)$ ,  $\text{Ar}(^1P_1, ^3P_1)$ , and  $\text{Kr}(^1P_1, ^3P_1)$  atoms by collisions with atomic and molecular quenchers measured in this experiment.

Quencher	Cross sections for deexcitation / $10^{-15} \text{ cm}^2$					
	$\text{Ne}(^1P_1)$	$\text{Ne}(^3P_1)$	$\text{Ar}(^1P_1)$	$\text{Ar}(^3P_1)$	$\text{Kr}(^1P_1)$	$\text{Kr}(^3P_1)$
Ar	$9.0 \pm 1.0, 9.0 \pm 0.5^a$					
Kr	$11 \pm 1, 11 \pm 1^a$					
Xe	$13 \pm 1, 13 \pm 1^a$					
$\text{N}_2$	$5.7 \pm 0.5$					
$\text{O}_2$	$12 \pm 1$					
CO	$6.9 \pm 0.3$					
NO	$7.6 \pm 0.3$					
$\text{CH}_4$	$9.0 \pm 0.7$					
$\text{C}_2\text{H}_4$	$(2.6 \pm 0.2)/2.4^b$					
<i>cyclo</i> - $\text{C}_3\text{H}_6$	$(2.4 \pm 0.1)/(1.8 \pm 0.1)^c$					
$\text{C}_3\text{H}_8$	$(18 \pm 1)/17^d$					
	$(12 \pm 1)/9.0^d$					
	$16 \pm 1$					
	$(15 \pm 1)/(14.4)^e$					
	$25 \pm 1$					
	$18 \pm 1$					
	$27 \pm 1$					
	$(22 \pm 2)/(14.7)^e$					
	$24 \pm 2$					
	$20 \pm 1$					

<sup>a</sup>The double entries for  $\text{Ne}(^1P_1)$ –Ar, Kr, and Xe mean the independent measurements.<sup>b</sup>Reference 10.<sup>c</sup>Reference 11.<sup>d</sup>Reference 12.<sup>e</sup>Reference 13.

of  $A^*$ , the oscillator strength for  $A \rightarrow A^*$  transitions, and the photoionization cross section of  $B$  at the excitation energy of  $A^*$ , i.e.,  $E^*$ , respectively.

In the deexcitation of an atom in a resonant state by a molecule, dissociative excitation transfer can occur together with Penning ionization,<sup>5,6</sup> i.e., the continuum absorption spectrum of the quencher molecule due to dissociation can exist at the photon energy of  $E^*$ , and hence there is a possibility that  $\sigma_{\text{WK}}$ , i.e., Eqs. (6)–(8) in which  $\sigma_i$  is replaced by the photoabsorption cross sections at  $E^*$ ,  $\sigma_a$ , might provide a better value of the total deexcitation cross section as mentioned in the introduction. In order to examine this idea the values of  $\sigma_{\text{M}}$  measured in the present and our

previous<sup>7,10,11,14–24</sup> experiments are compared with the values of  $\sigma_{\text{WKI}}$  and  $\sigma_{\text{WKA}}$  calculated using  $\sigma_i$  and  $\sigma_a$ , respectively. The values of  $\sigma_{\text{WKI}}$  and  $\sigma_{\text{WKA}}$  are recalculated using more reliable data sets for  $\sigma_i$  and  $\sigma_a$ <sup>25–38</sup> for some collision systems we investigated before. We note that  $\sigma_{\text{WKI}}$  and  $\sigma_{\text{WKA}}$  in Eq. (6) are velocity averaged with the Maxwellian distribution of  $v$ , which is needed to compare with  $\sigma_{\text{M}}$  obtained from  $k_{\text{M}}$  according to Eq. (5). Let us use the same symbols,  $\sigma_{\text{WKI}}$  and  $\sigma_{\text{WKA}}$ , also for the averaged cross sections.

In Fig. 2(a),  $\sigma_{\text{M}}$  for  $\text{He}(2^1P)$ ,  $\text{Ne}(^1P_1)$ ,  $\text{Ar}(^1P_1)$ , and  $\text{Kr}(^1P_1)$ –M systems divided by  $\sigma_{\text{WKI}}$  are plotted against the photoionization quantum yields,  $\eta$  ( $\equiv \sigma_i/\sigma_a$ ), of the

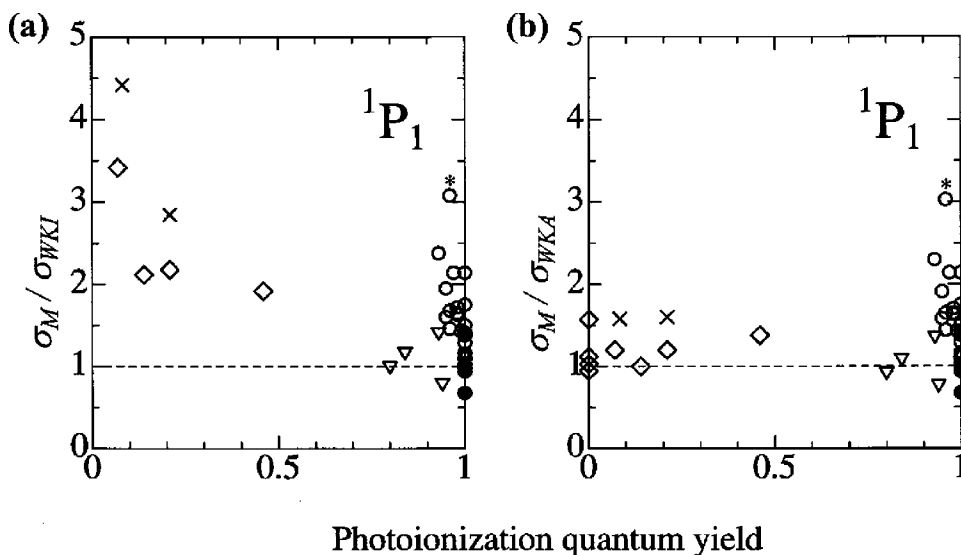


FIG. 2. The ratio of the measured cross sections,  $\sigma_{\text{M}}$ , to the WK cross sections,  $\sigma_{\text{WKI}}$  and  $\sigma_{\text{WKA}}$ , at room temperature for deexcitation of  $\text{He}(2^1P)$  atom by collisions with atoms (●) and molecules (○), of the lowest excited  $\text{Ne}(^1P_1)$  atom by atoms (△) and molecules (▽), of the lowest excited  $\text{Ar}(^1P_1)$  atom by molecules (◇), and of the lowest excited  $\text{Kr}(^1P_1)$  atom by molecules (×) as a function of the photoionization quantum yields,  $\eta$ , of the quencher atoms or molecules at the excitation energies of the excited rare gas atoms. (a)  $\sigma_{\text{M}}/\sigma_{\text{WKI}}$  vs  $\eta$  and (b)  $\sigma_{\text{M}}/\sigma_{\text{WKA}}$  vs  $\eta$ . See Sec. III as to  $\sigma_{\text{WKI}}$  and  $\sigma_{\text{WKA}}$ . The cross sections for deexcitation,  $\sigma_{\text{M}}$ , are from the present and our previous (Refs. 7, 14–23) experiments. The photoionization cross sections, photoabsorption cross sections, and photoionization quantum yields in use are obtained from Refs. 25–35. The points labeled “\*” correspond to  $\text{He}(2^1P)$ – $\text{Si}_2\text{H}_6$  system (see Sec. III).

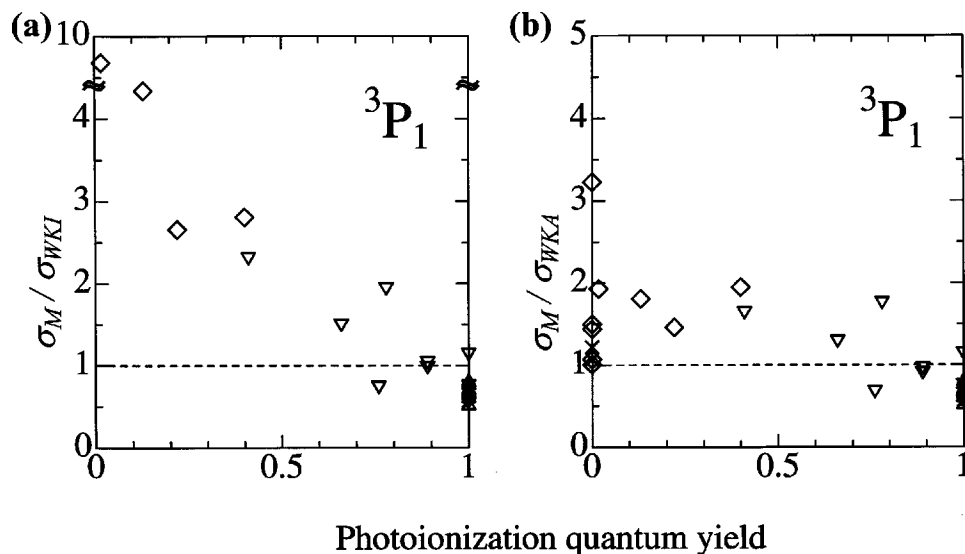


FIG. 3. The ratio of the measured cross sections,  $\sigma_M$ , to the WK cross sections,  $\sigma_{WKI}$  and  $\sigma_{WKA}$ , at room temperature for deexcitation of the lowest excited Ne( $^3P_1$ ) atom by collisions with atoms ( $\Delta$ ) and molecules ( $\nabla$ ), of the lowest excited Ar( $^3P_1$ ) atom by molecules ( $\diamond$ ), and of the lowest excited Kr( $^3P_1$ ) atom by molecules ( $\times$ ) as a function of the photoionization quantum yields,  $\eta$ , of the quencher atoms or molecules at the excitation energies of the excited rare gas atoms. (a)  $\sigma_M/\sigma_{WKI}$  vs  $\eta$  and (b)  $\sigma_M/\sigma_{WKA}$  vs  $\eta$ . See Sec. III as to  $\sigma_{WKI}$  and  $\sigma_{WKA}$ . The cross sections for deexcitation,  $\sigma_M$ , are from the present and our previous (Refs. 7, 10, 11, 14, 18, 23, and 24) experiments. The photoionization cross sections, photoabsorption cross sections, and photoionization quantum yields in use are obtained from Refs. 25–32 and 34–38.

quenchers, M, at the excitation energies of the excited rare gas atoms. In the region of  $\eta$  near unity, the values of  $\sigma_M$  for Ne( $^1P_1$ ), Ar( $^1P_1$ ), and Kr( $^1P_1$ ) atoms are in good agreement with those of  $\sigma_{WKI}$  while in the smaller region of  $\eta$  the discrepancy between  $\sigma_M$  and  $\sigma_{WKI}$  becomes larger. In Fig. 2(b), the values of  $\sigma_M/\sigma_{WKA}$  are plotted against  $\eta$  for the same collision systems as in Fig. 2(a). It seems that  $\sigma_{WKA}$  reproduces  $\sigma_M$  better than  $\sigma_{WKI}$  in the region of  $\eta$ ,  $0 < \eta \leq 1$ , except for some of He( $2^1P$ )–molecule systems ( $\circ$ ), in particular He( $2^1P$ )–Si<sub>2</sub>H<sub>6</sub> system, for which  $\sigma_M/\sigma_{WKI}$  and  $\sigma_M/\sigma_{WKA}$  amount to 3 (see the points labeled “\*” in Fig. 2). Such remarkable discrepancy seen in He( $2^1P$ )–molecule systems seems to be attributed to the bent trajectories caused by the attractive part of the interaction potential that is neglected in the WK theory, as pointed out before.<sup>22</sup>

In Fig. 2(b) the values of  $\sigma_M/\sigma_{WKA}$  are also plotted for the systems in which Penning ionization cannot occur energetically, i.e., those of  $\eta(E^*)$  are zero since  $E^*$  is lower than the ionization potential of M. It seems that  $\sigma_{WKA}$  reproduces  $\sigma_M$  well even in the case that Penning ionization cannot occur (see also Ref. 7). We note that the original WK theory does not deal with such a case.

In conclusion it follows from Fig. 2 that  $\sigma_{WKA}$  for an excited rare gas atom in the  $^1P_1$  state reproduces  $\sigma_M$  better than  $\sigma_{WKI}$  in the whole region of  $\eta$ ,  $0 \leq \eta \leq 1$ , although there are some exceptions. The validity of the extended WK theory has been confirmed experimentally, and then let us discuss this validity from a theoretical point of view. In the WK theory, Penning ionization takes place through the dipole–dipole interaction, and the basic equation for the time-evolution of the initial state includes the product of the two transition dipole matrix elements squared as an important part. This can be obtained providing that the interaction matrix element from the initial state to the final continuum-state

is not strongly dependent on the energy of the final continuum-state, i.e., they assumed that it is constant within an energy-width determined by the collision time and the uncertainty principle. In the treatment, the dipole–dipole interaction is determined by the dipolar electron transitions. In this sense, the transition dipoles should be taken as those for photoabsorption and not as those for photoionization. We also note that the final continuum-states need not be ionized states and that they can be any kind of continuum states, e.g., vibrational ones.<sup>7,39</sup> It seems from the above discussion that the extended WK theory, i.e.,  $\sigma_{WKA}$ , takes account of both Penning ionization and dissociative excitation transfer, the former corresponds to the final continuum-states in electronic motion and the latter to those in vibrational motion.

In Fig. 3,  $\sigma_M/\sigma_{WKI}$  and  $\sigma_M/\sigma_{WKA}$  are plotted against  $\eta$  for Ne( $^3P_1$ ), Ar( $^3P_1$ ), and Kr( $^3P_1$ )–M systems, and show almost the same features as in Fig. 2. The values of  $\sigma_{WKA}$  for Ne and Ar in the  $^3P_1$  state, however, do not reproduce those of  $\sigma_M$  so well as the values of  $\sigma_{WKA}$  for Ne and Ar in the  $^1P_1$  state do in Fig. 2(b). This seems to be attributed to the fact that the oscillator strengths for Ne( $^1S_0 \rightarrow ^3P_1$ ), 0.010, and for Ar( $^1S_0 \rightarrow ^3P_1$ ), 0.051, are much smaller than the oscillator strengths for Ne( $^1S_0 \rightarrow ^1P_1$ ), 0.15, and for Ar( $^1S_0 \rightarrow ^1P_1$ ), 0.25, respectively.<sup>8</sup> The smaller oscillator strengths result in the decreasing role of the dipole–dipole interaction and the increasing role of the electron-exchange interaction in the deexcitation processes, the latter of which is not taken into account in the WK theory. On the other hand, the oscillator strength for Kr( $^1S_0 \rightarrow ^3P_1$ ), 0.15, is as large as the oscillator strength for Kr( $^1S_0 \rightarrow ^1P_1$ ), 0.14, which is consistent with our finding that the values of  $\sigma_M$  for Kr( $^3P_1$ )–M coincide with  $\sigma_{WKA}$  as well as those of  $\sigma_M$  for Kr( $^1P_1$ )–M do.

The results of the comparison between the experiments



and the WK theory in Figs. 2 and 3 depend on the data sets for the photoionization and photoabsorption cross sections in use, which are, strictly speaking, influenced by the experimental problems such as the energy resolution, the calibration of photon energy, the normalization procedure to obtain the absolute values of the cross sections and so forth.<sup>25,26</sup> Hence we have carefully chosen the data sets<sup>25–38</sup> in terms of the points mentioned above and note that Figs. 2 and 3 show the gross but substantial features.

#### IV. CONCLUSION

It is observed experimentally that the WKA cross sections,  $\sigma_{\text{WKA}}$ , reproduce the measured cross sections for de-excitation,  $\sigma_{\text{M}}$ , of Ne, Ar, and Kr atoms in the lowest excited  $^1P_1$  state by collisions with a wide range of atoms and molecules at room temperature better than the WKI cross sections,  $\sigma_{\text{WKI}}$ . Almost the same features are seen for Ne, Ar, and Kr atoms in the lowest excited  $^3P_1$  state. The values of  $\sigma_{\text{WKA}}$  for Ne and Ar atoms in the  $^3P_1$  state, however, do not reproduce  $\sigma_{\text{M}}$  so well as  $\sigma_{\text{WKA}}$  for Ne and Ar atoms in the  $^1P_1$  state does while  $\sigma_{\text{WKA}}$  for the Kr( $^3P_1$ ) atom reproduces  $\sigma_{\text{M}}$  as well as  $\sigma_{\text{WKA}}$  for the Kr( $^1P_1$ ) atom does. Based on the experimental findings mentioned above we have concluded that the extended WK theory, Eqs. (6)–(8) where  $\sigma_i$  in Eq. (8) is replaced by  $\sigma_a$ , is as valuable for the evaluation of the cross sections for deexcitation of excited rare gas atoms (Ne, Ar, and Kr) in resonant states by molecules as the original WK theory is for the evaluation of the cross sections for deexcitation by atoms.

#### ACKNOWLEDGMENT

The authors would like to thank Professor Tsutomu Watanabe for critical and helpful discussion.

<sup>1</sup>T. Watanabe and K. Katsuura, J. Chem. Phys. **47**, 800 (1967).

<sup>2</sup>Y. Hatano, in *Pulse Radiolysis*, edited by Y. Tabata (CRC, Boca Raton, 1991), pp. 199–228.

<sup>3</sup>Y. Hatano, Radiat. Phys. Chem. **34**, 675 (1989).

<sup>4</sup>M. Ukai and Y. Hatano, in *Gaseous Electronics and Its Applications*, edited by R. W. Crompton, M. Hayashi, D. E. Boyed, and T. Makabe (Kluwer Academic, Dordrecht, 1991), pp. 51–72.

<sup>5</sup>Y. Hatano, Adv. At., Mol., Opt. Phys. **43**, 231 (2000).

<sup>6</sup>Y. Hatano, Phys. Rep. **313**, 109 (1999).

<sup>7</sup>M. Ukai, H. Koizumi, K. Shinsaka, and Y. Hatano, J. Chem. Phys. **84**, 3199 (1986).

<sup>8</sup>A. A. Radzig and B. M. Smirnov, *Reference Data on Atoms, Molecules, and Ions* (Springer-Verlag, Berlin, 1985).

<sup>9</sup>S. G. Lias, J. E. Bartmess, J. F. Liebman, J. L. Holmes, R. D. Levin, and W. G. Mallard, J. Phys. Chem. Ref. Data, Suppl. 1, **17**, 1 (1988).

<sup>10</sup>A. Yokoyama and Y. Hatano, Chem. Phys. **63**, 59 (1981).

<sup>11</sup>H. Yoshida, M. Kitajima, H. Kawamura, K. Hidaka, M. Ukai, N. Kouchi, and Y. Hatano, J. Chem. Phys. **98**, 6190 (1993).

<sup>12</sup>G. S. Hurst, E. B. Wagner, and M. G. Payne, J. Chem. Phys. **61**, 3680 (1974).

<sup>13</sup>V. A. Alekseev and D. W. Setser, J. Phys. Chem. A **103**, 4016 (1999).

<sup>14</sup>H. Yoshida, H. Kawamura, M. Ukai, N. Kouchi, and Y. Hatano, J. Chem. Phys. **96**, 4372 (1992).

<sup>15</sup>M. Ukai, Y. Tanaka, H. Koizumi, K. Shinsaka, and Y. Hatano, J. Chem. Phys. **84**, 5575 (1986).

<sup>16</sup>M. Ukai, H. Nakazawa, K. Shinsaka, and Y. Hatano, J. Chem. Phys. **88**, 3623 (1988).

<sup>17</sup>M. Ukai, H. Yoshida, Y. Morishima, H. Nakazawa, K. Shinsaka, and Y. Hatano, J. Chem. Phys. **90**, 4865 (1989).

<sup>18</sup>M. Ukai, N. Suzuki, K. Shinsaka, and Y. Hatano, J. Chem. Soc. Jpn. **1989**, 1188 (in Japanese).

<sup>19</sup>H. Yoshida, Y. Morishima, M. Ukai, K. Shinsaka, N. Kouchi, and Y. Hatano, Chem. Phys. Lett. **176**, 173 (1991).

<sup>20</sup>Y. Morishima, H. Yoshida, M. Ukai, K. Shinsaka, N. Kouchi, and Y. Hatano, J. Chem. Phys. **94**, 2564 (1991).

<sup>21</sup>Y. Morishima, H. Yoshida, M. Ukai, K. Shinsaka, N. Kouchi, and Y. Hatano, J. Chem. Phys. **97**, 3180 (1992).

<sup>22</sup>H. Yoshida, M. Ukai, H. Kawamura, N. Kouchi, and Y. Hatano, J. Chem. Phys. **97**, 3289 (1992).

<sup>23</sup>H. Yoshida, Ph. D. thesis, Tokyo Institute of Technology, 1992.

<sup>24</sup>D. B. Khadka, Y. Fukuchi, M. Kitajima, K. Hidaka, N. Kouchi, Y. Hatano, and M. Ukai, J. Chem. Phys. **107**, 2386 (1997).

<sup>25</sup>K. Kameta, N. Kouchi, and Y. Hatano, in *Photon and Electron Interactions with Atoms, Molecules and Ions*, Landolt-Börnstein, edited by Y. Itikawa (Springer-Verlag), Vol. I/17C, Chap. 4 (to be published).

<sup>26</sup>K. Kameta, N. Kouchi, M. Ukai, and Y. Hatano, J. Electron Spectrosc. Relat. Phenom. **123**, 225 (2002).

<sup>27</sup>K. Watanabe, F. M. Matsunaga, and H. Sakai, Appl. Opt. **6**, 391 (1967).

<sup>28</sup>R. E. Rebbert and P. Ausloos, J. Res. Natl. Bur. Stand., Sect. A **75A**, 481 (1971).

<sup>29</sup>J. A. R. Samson and J. L. Gardner, J. Electron Spectrosc. Relat. Phenom. **8**, 35 (1976).

<sup>30</sup>J. A. R. Samson, G. N. Haddad, and J. L. Gardner, J. Phys. B **10**, 1749 (1977).

<sup>31</sup>J. A. R. Samson, J. L. Gardner, and G. N. Haddad, J. Electron Spectrosc. Relat. Phenom. **12**, 281 (1977).

<sup>32</sup>J. A. R. Samson and L. Yin, J. Opt. Soc. Am. B **6**, 2326 (1989).

<sup>33</sup>K. Kameta, M. Ukai, T. Numazawa, N. Terazawa, Y. Chikahiro, N. Kouchi, Y. Hatano, and K. Tanaka, J. Chem. Phys. **99**, 2487 (1993).

<sup>34</sup>T. N. Olney, N. M. Cann, G. Cooper, and C. E. Brion, Chem. Phys. **223**, 59 (1997).

<sup>35</sup>K. Kameta (private communication):  $\sigma_i$ ,  $\sigma_a$ , and  $\eta$  of C<sub>2</sub>H<sub>4</sub>.

<sup>36</sup>J. W. Raymond and W. T. Simpson, J. Chem. Phys. **47**, 430 (1967).

<sup>37</sup>C. E. Klotz, J. Chem. Phys. **56**, 124 (1972).

<sup>38</sup>D. A. Shaw, D. M. P. Holland, M. A. MacDonald, A. Hopkirk, M. A. Hayes, and S. M. McSweeney, Chem. Phys. **163**, 387 (1992).

<sup>39</sup>T. Oka, M. Kogoma, M. Imamura, S. Arai, and T. Watanabe, J. Chem. Phys. **70**, 3384 (1979).